Rubber Modeling Using Uniaxial Test Data

G. L. BRADLEY,[1] P.C. CHANG,[2] G. B. MCKENNA[3]

[1] Alvi Associates, Inc., Towson, Maryland 21204

[2] Department of Civil engineering, University of Maryland, College Park, Maryland 20742

[3] Department of Chemical Engineering, Texas Tech University, Lubbock, Texas 79409-3121

Received 8 March 2000; accepted 17 May 2000

ABSTRACT: Accurate modeling of large rubber deformations is now possible with finite-element codes. Many of these codes have certain strain-energy functions built-in, but it can be difficult to get the relevant material parameters and the behavior of the different built-in functions have not been seriously evaluated. In this article, we show the benefits of assuming a Valanis–Landel (VL) form for the strain-energy function and demonstrate how this function can be used to enlarge the data set available to fit a polynomial expansion of the strain-energy function. Specifically, we show that in the ABAQUS finite-element code the Ogden strain-energy density function, which is a special form of the VL function, can be used to provide a planar stress–strain data set even though the underlying data used to determine the constants in the strain-energy function include only uniaxial data. Importantly, the polynomial strain-energy density function, when fit to the uniaxial data set alone, does not give the same planar stress–strain behavior as that predicted from the VL or Ogden models. However, the polynomial form does give the same planar response when the VL-generated planar data are added to the uniaxial data set and fit with the polynomial strain-energy function. This shows how the VL function can provide a reasonable means of estimating the three-dimensional strain-energy density function when only uniaxial data are available. © 2001 John Wiley & Sons, Inc. J Appl Polym Sci 81: 837–848, 2001

Key words: earthquake bearing; finite element analysis; mechanical properties; Mooney–Rivlin material; Ogden function; Rivlin expansion; rubber; strain energy function; Valanis–Landel function

INTRODUCTION

Elastomeric bearings used for earthquake load isolation consist of alternating layers of steel and rubber—the latter vulcanized under high temperature—to form a composite bearing. Under axial loading, the rubber in the bearing expands outward. This deformation leads to the rupture of steel in the radial direction or debonding between steel and rubber. In prior work, the load-deflection response of such a bearing was modeled using the ABAQUS[1] finite-element code.[2] In this article, we present the methodology used to determine the parameters employed in the constitutive model for the rubber used in that study.

Most finite-element codes today include a hyperelastic constitutive model for analysis. In the

Correspondence to: G. B. McKenna (greg.mckenna@coe.ttu.edu).

Contract grant sponsor: Building and Fire Research Laboratory and Materials Science and Engineering Laboratory, National Institute of Standards and Technology, Gaithersburg, MD.

Journal of Applied Polymer Science, Vol. 81, 837–848 (2001)

case of the ABAQUS version available at the time of the current work, the hyperelastic models included were a multiterm Rivlin expansion and a multiterm version of the Ogden model. Both include the possibility of material compressibility. A major difficulty in the use of such finite-element codes is the experimental determination of the material parameters to use in the model chosen for calculation. For the polynomial expansion in the invariants of the deformation tensor, the experimental data needed include uniaxial, biaxial, and planar extension (pure shear) tests. Uniaxial deformations include both tensile and compressive deformations. Yet, it is typical that only uniaxial tension tests are performed and this may lead to limited accuracy when attempting to determine the strain-energy density function. In particular, the exclusion of compression data may result in a strain-energy density function that does not capture much of the strain energy's dependence on I_2. For this reason, tests were performed in both tension and compression.

Furthermore, measurements of pure shear or nonequal biaxial responses to obtain additional data, which would improve the performance of the polynomial model in the full range of deformation geometries, requires special mechanical devices that are expensive to make and not always practicable to build. In this article, we show that one possible and practical alternative to performing the pure shear (or other) tests is to use the Valanis–Landel (VL) function[3] to generate such data from experimental uniaxial tension and compression data alone. An important point that is made in the article is that, to the extent that the VL function is valid, it provides a means to estimate deformations other than uniaxial tension and compression that differ from those estimated from the polynomial form of the strain-energy function when the latter is fitted to the same set of uniaxial data. The polynomial form, when fitted to uniaxial tension, uniaxial compression, and the VL-generated pure shear data, gives good fits to the entire data set. This result suggests the need to adequately consider more than just uniaxial data when computing strain-energy functions for rubber. Finally, in the work here, we describe the use of a compressible strain-energy function. The use of such a function is important in earthquake bearings because the high pressures involved in their loading can lead to as much as 10% vol change in the rubber.

CONSTITUTIVE MODELING OF RUBBER

General Considerations

Rubber is a nonlinear, nearly elastic material even at large strains. Such behavior is well characterized by a hyperelastic model. Here, we assume that the rubber is isotropic; hence, the strain-energy density function can be written as a function of the strain invariants I_1; $U = (I_1, I_2, I_3)$, where I_3 is the square of the volume ratio J ($J = \sqrt{I_3}$) and is equal to 1 for a perfectly incompressible material. It is common to assume that rubber materials are incompressible when the material is not subjected to large hydrostatic loadings. However, in the case here, large hydrostatic stresses arise in the compressive loading of the earthquake bearings and we need to consider both the compressible and the incompressible problems.

Practically, solid rubber has a Poisson's ratio that ranges from 0.49 to 0.50.[4] As described subsequently, the Poisson's ratio for the rubber used in this study was found by a volumetric compression test to be 0.4994. Hence, the rubber is nearly incompressible. If a material is incompressible, the hydrostatic stress cannot be found from the displacements, since the application of a hydrostatic stress results in no deformation. "Mixed" formulations have successfully dealt with this problem.[5,6] In a mixed formulation for a perfectly incompressible material, the internal energy is augmented by adding the term $p(J - 1)$, where p is a Lagrange multiplier (the hydrostatic stress) introduced to impose the constraint $J - 1 = 0$ ($J - 1$ is the volumetric strain). This allows the hydrostatic stress to be approximated directly, independent of the displacements. The stress that is derived from the displacements is the deviatoric stress. The sum of the hydrostatic and deviatoric stress tensors gives the total stress tensor. We note that this is an approximation, as Penn[7] and Fong and Penn[8] showed deviations from such a separability of deviatoric and hydrostatic components in measurements of volume changes in rubber under large uniaxial deformations.

Following the development in ABAQUS,[1] the deviatoric portion of the strain energy can be written using revised invariants that remove any effect due to volume change. The strain energy is written as

$$U = U(\bar{I}_1, \bar{I}_2, I_3) = \bar{U}(\bar{I}_1, \bar{I}_2) + \tilde{U}(I_3) \qquad (1)$$

where the bars over the first two strain invariants indicate removal of volume changes.

The decoupling of the deviatoric and volumetric strain energy can only be valid if the bulk modulus is a constant (Sussman and Bathe,[9] but see also Penn[7] and Fong and Penn,[8] cited above). A constant bulk modulus implies that the pressure/volume ratio is constant. Results of volumetric testing, discussed later, show that the bulk modulus is a constant, independent of the applied uniaxial compressive deformation. On this basis, the decoupling of the strain energy into deviatoric and volumetric portions is assumed to be a reasonable approximation for the rubber tested and, therefore, the use of the mixed approach is justified.

Two forms of the strain-energy density function based on the mixed formulation were used. The first is the polynomial strain energy density function, in which the strain energy is

$$U = \sum_{i+j=1}^{N} C_{ij}(\bar{I}_1 - 3)^i(\bar{I}_2 - 3)^j + \sum_{i=1}^{N} \frac{1}{D_i}(J_{el} - 1)^{2i} \tag{2}$$

The first summation is the contribution due to deviatoric effects, and the second summation is the contribution due to volumetric effects. The C_{ij} and D_i are parameters that are found from the rubber test data and $\bar{I}_1$ and $\bar{I}_2$ are the first and second invariants of the Cauchy–Green deformation tensor with the volume change removed. J_{el} is the ratio of the current volume to the original volume excluding thermal effects. For $N = 1$, the deviatoric contribution to the strain energy is called the Mooney–Rivlin function. It is often written as

$$U = C_{10}(\bar{I}_1 - 3) + C_{01}(\bar{I}_2 - 3) \tag{3}$$

In addition to the well-known invariant expansion described above, the strain-energy density function of an isotropic elastic material can also be written in terms of the stretches λ. Valanis and Landel[3] postulated that the strain-energy density function is a function that is separable in terms of the principal stretches, and the total strain energy is

$$U = u(\lambda_1) + u(\lambda_2) + u(\lambda_3) \tag{4}$$

We will refer to $u(\cdot)$ as the Valanis–Landel or VL function.

In ABAQUS, a special form of the VL function for the strain-energy density is provided—it is the Ogden strain-energy density function, which we also consider in this study. The contribution due to deviatoric effects is written as a function of the stretch ratios. In ABAQUS, a compressible form of the Ogden function is also provided and the contribution due to volumetric effects is the same as that used for the polynomial strain-energy function:

$$U = \sum_{i=1}^{N} \frac{2\mu_i}{\alpha_i^2}(\bar{\lambda}_1^{\alpha_i} + \bar{\lambda}_2^{\alpha_i} + \bar{\lambda}_3^{\alpha_i} - 3) + \sum_{i=1}^{N} \frac{1}{D_i}(J_{el} - 1)^{2i} \tag{5}$$

In eq. (5), μ_i, α_i, and D_i are parameters that are found from the rubber test data. The principal stretch ratios $\bar{\lambda}_k^{\alpha_i}$ have the volume change removed. To determine the deviatoric parameters C_{ij} in eq. (3) and μ_i and α_i in eq. (5), experimental data can be fitted to one or more of the three deformation modes: uniaxial (tension or compression), equibiaxial (tension or compression), and planar (tension or compression; this is pure shear when the material is incompressible).[1] We remark further that the C_{ij} and the μ_i and α_i, are assumed to be independent of the volume.

Using a right-handed Cartesian coordinate system with axes x_1, x_2, and x_3, let the uniaxial deformation mode correspond to an application of force along the longitudinal axis of the specimen. For the purpose of explanation here, we denote this axis x_1. Then, the specimen is free to expand or contract along axes x_2 and x_3. The equibiaxial deformation mode corresponds to equal stretches along the x_1 and x_2 axes, with unrestrained movement along the x_3 axis. Planar deformation corresponds to a stretch along the x_1 axis, with no stretch allowed along the x_2 axis, and unrestrained movement along the x_3 axis. Each of these modes is an example of a deformation in which the directions of principal strain do not change, that is, the deformations take place along the principal axes. Each mode can be written in terms of a single stretch, which allows the stress–strain relationship to be easily measured. To determine the isotropic (or hydrostatic) parameters in D_i in eqs. (2) and (4), constrained compression tests in which volume change could be measured were performed.

For an incompressible material, uniaxial compression is equivalent to equibiaxial tension, uniaxial tension is equivalent to equibiaxial compression, and planar tension is equivalent to planar compression. For the material analysis performed here, experimental testing was performed in uniaxial tension and uniaxial compression. A planar test could have been done had the appropriate equipment been available and may have captured dependence on the strain invariants that was missed by the uniaxial tests. Unfortunately, this experiment requires more extensive preparation and tooling than was available in our laboratories. In lieu of an actual planar test, the stress–strain response in planar tension was calculated using the VL function, which has been shown to be an excellent descriptor of actual rubber behavior.[10–13]

Determination of the VL Strain-energy Function

As noted above, apart from the constrained compression, the mechanical testing of the rubber was performed only in the uniaxial tensile and compressive modes. The planar deformation mode is independent of either of the uniaxial tension or uniaxial compression modes. No planar deformation tests were done, since a test apparatus for this mode of deformation was neither available nor practicable to build for small specimens. Planar deformation is also referred to as a pure shear or strip biaxial deformation. It is different from simple shear deformation in that the principal strain directions remain unchanged during the deformation. Because of the lack of test data and the known success of the VL function in describing the behavior of rubber (see references cited above), we used the VL function to generate stress data for planar deformation as if the tests had been performed.

Kearsley and Zapas[13] showed how to obtain the VL function from uniaxial tensile and compressive data, which we did obtain. In terms of the true stress t and the stretch λ, the following recursive expression can be used to obtain the derivative $u'(\lambda)$ of the VL function:

$$\lim_{n\to\infty} \sum_{k=0}^{n-1} [t(\lambda^{(1/4)^k}) + t(\lambda^{-(1/2)(1/4)^k})] = \lambda u'(\lambda) \quad (6)$$

The right-hand side of eq. (6) is an infinite sum of the true stresses at the stretches specified in the bracketed expression. The rapid convergence of this infinite series allows one to obtain the VL function with a small number of terms. Note that the first and second terms are on opposite sides of the undeformed state ($\lambda = 1$), so that both extension and compression data are required, and the terms of the series converge rapidly from both sides of the undeformed state. A computer program was written to find the values $\mu'(\lambda)$ at the desired stretch values. The formula for uniaxial engineering stresses, written in terms of the derivative of the VL function, is

$$\sigma = u'(\lambda) - \lambda^{-3/2}u'(\lambda^{-1/2}) \quad (7)$$

EXPERIMENTAL

Materials

The material used in this study was a carbon black-reinforced rubber compound of the same composition as that used in the manufacture of the elastomeric bearings. It was provided in the form of sheets provided by the bearing manufacturer and prepared according to ASTM D3182-89.[14] Nominal rubber mechanical properties provided by the manufacturer are presented in Table I.

Mechanical Testing Procedures

All rubber testing was performed on an Instron 1125 test machine. The accuracy of this machine was established through a calibration test using known dead loads and was calibrated according to ASTM E4, which requires that the machine reading be within 1% of the true reading. The machine met these requirements. This is equivalent to a relative expanded uncertainty ($k = 2$) of 1% and is small compared to specimen variability for the rubber uniaxial testing.

The uniaxial tension tests were performed up to engineering tensile strains of 6.00, very near the ultimate elongation of the rubber, to ensure that the strain-energy density function would adequately represent the severe engineering tensile stresses and strains expected in the finite-element analysis of the elastomeric bearings. The testing was performed on 14 dumbbell specimens. The variation about the mean of these tests was approximately $\pm 10\%$, so the variability can be attributed to factors outside the resolution of the testing machine. Sources of variation include (1) differences in the properties of the rubber and (2) measurement error. Displacements were recorded manually using a hand-held caliper, and

Table I Nominal Mechanical Properties of the Rubber Supplied by the Elastomeric Bearing Manufacturer and Tested for This Study

Material	Shear Modulus [ASTM D-4014-89, Annex A1] MPa (psi)	Tensile Strength [ASTM D-412-92, Method A] MPa (psi)	Ultimate Elongation [ASTM D-412-92, Method A] (%)	Compression Set [ASTM D-395-89, Method B[15]] (%)
Manufacturer supplied composite batch	0.883 (128)	16.59 (2406)	621	20.75

force readings were manually taken at the time of each displacement reading. Measurement error in the cross-sectional area can also affect the results. Based on this limited testing sample and manual testing methodology, it is difficult to say how much of the variability is due strictly to differences in the properties of the rubber, but it is likely that the largest portion of the variability is due to the manual measurement process. Testing of the rubber was performed at strain rates ranging from 5×10^{-4} to 4.4×10^{-2} s^{-1}. There was no trend of the data with the strain rate and the test results reported here are for the strain rate of 5×10^{-4} s^{-1} (see Bradley[2]).

The uniaxial compressive tests were carried to a stress level exceeding 100 MPa. At this stress level, the engineering compressive strain exceeded 0.85. To get accurate displacement readings for the compression test, machine compliance was removed from the displacement data. The uniaxial compression test was made to simulate homogeneous compression, in which straight lines before deformation remain straight after deformation. This test requires the loaded ends of the specimen to slide freely along the loaded surface, so there is no bowing of the unloaded surface. Attaining perfect homogeneous compression requires a frictionless contact between the platen and the sample surface. This condition was approximated by applying a lubricant to the specimen's plane faces.

Whether or not bowing of the unloaded surfaces occurred was very difficult to determine visually because the loaded specimens became very thin and the lubricant squeezing out from the edges of the loaded surfaces obscured the view. After unloading, the circle of lubricant on the platen showed that the loaded surface had slipped considerably. To assure ourselves that, in fact, the specimens were not bowing very much, we tested two specimens in compression, one with a shape factor of 0.55 and the other with a shape factor of 1.10. The shape factor, S, is a measure of the relative thickness of a specimen. It is defined as the ratio of the area of one loaded surface to the area of the unloaded surface. For cylindrical specimens, $S = r/2T$, where r is the radius and t is the thickness of the specimen. The responses were nearly identical after removal of the machine compliance. Since the stress–strain response is a strong function of the shape factor for bonded specimens[16,17] and is independent of shape factor for homogeneous compression, this result gives us confidence that the compression test was a fairly good representation of homogeneous compression. For the two compression tests done, the variation of the test values about the mean of the two tests was approximately $\pm 2.8\%$.

Three volumetric tests were performed, each using a cylindrical compression-set rubber specimen, using a device manufactured for this experiment. It consists of two steel plates joined together by cap screws, with a hole cut into the upper plate. The diameter of the hole is 1.100 in., with tolerances of -0.000 and $+0.001$ in. A piston, to which compressive load was applied, was cut to a diameter of 1.100 in. with tolerances of $+0.000$ and -0.001 in. The tight tolerances were necessary because of the extreme importance of providing no room for the rubber to extrude during the test. The piston slid freely through the hole when the bottom plate was removed, but with the bottom plate attached, entrapped air retarded its movement considerably, showing that the device and sample diameters are identical. After removal of the machine compliance, the raw data were converted into a pressure and volume ratio.

RESULTS

Figure 1 depicts the experimentally determined uniaxial tensile and compressive stress–strain data (crosses). These data were used to determine the deviatoric constants in the strain-energy den-

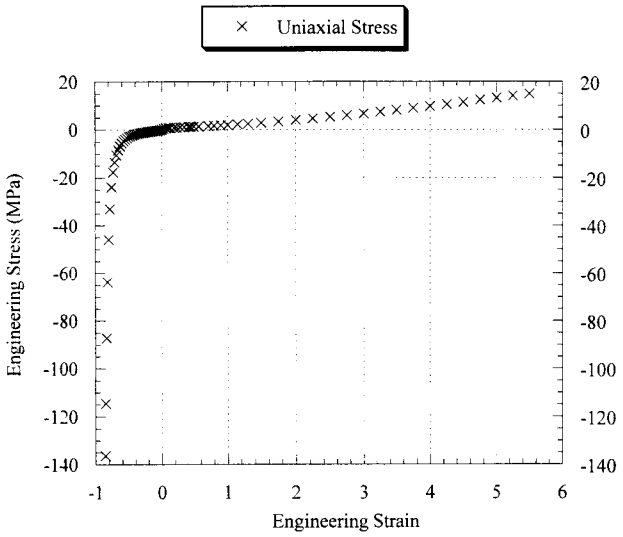

Figure 1 Plot of the uniaxial stress–strain behavior of the filled rubber: (×) experimental data; (solid line) VL fit to the data.

sity functions and to determine the VL function (solid line), both of which were used in the finite-element modeling [see eqs. (2), (4), (5), and (7)]. Figure 2 shows the results of the constrained compression test. These data confirm the constancy of the bulk modulus and justify the approximation involved in decomposing the strain-energy density function into a deviatoric and a hydrostatic component [see eqs. (1), (2), and (4)]. Additionally, these data were used to determine the hydrostatic (or volumetric) constants in the strain-energy density functions, which were then

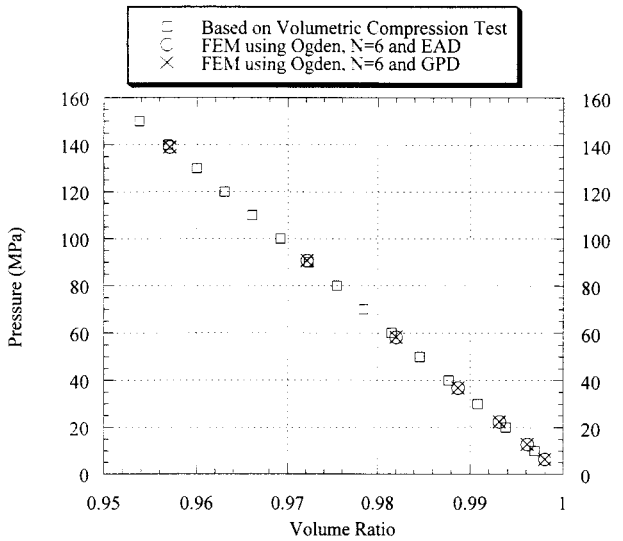

Figure 2 Comparison of volumetric compression test results and finite-element results for filled rubber.

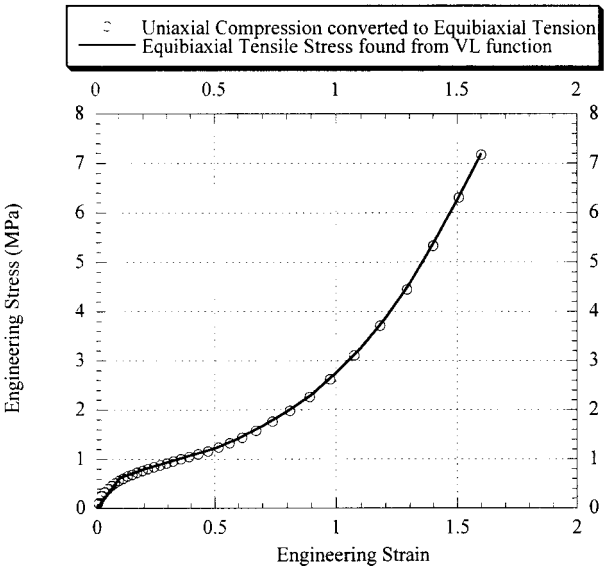

Figure 3 Comparison of the equibiaxial stress–strain behavior of the filled rubber determined from eqs. (8) and (9).

used in the finite-element modeling. For the three volumetric tests, the slopes of each graph, which correspond to the bulk modulus, differ by only ±0.86% from the mean value. This difference cannot be attributed to any specific errors in testing or differences in the bulk modulus from sample to sample because they are within the resolution of the testing machine.

The data of Figures 1 and 2 permit the determination of the compressible VL function parameters. The solid line in Figure 1 is the VL function fit to the uniaxial tension and compression data [crosses in Fig. 1; also see eq. (7)]. Clearly, the VL function provides an excellent fit to the uniaxial stress–strain data.

As another check on the stresses generated by the VL function, we compare equibiaxial stresses generated in two different ways, as follows: First, uniaxial compression and equibiaxial tension are equivalent for an incompressible material. Through a simple transformation, one can show that the equibiaxial stress–strain, written as a function of uniaxial compression and the stretch, is

$$\sigma_{\text{equibiaxial}} = -\sigma_{\text{compressive}}\lambda^{3/2} \tag{8}$$

and, second, in terms of the VL function, the equibiaxial stress–strain relationship can be expressed as follows:

$$\sigma_{\text{equibiaxial}} = u'(\lambda) - \frac{1}{\lambda^3}\,u'\left(\frac{1}{\lambda^2}\right) \tag{9}$$

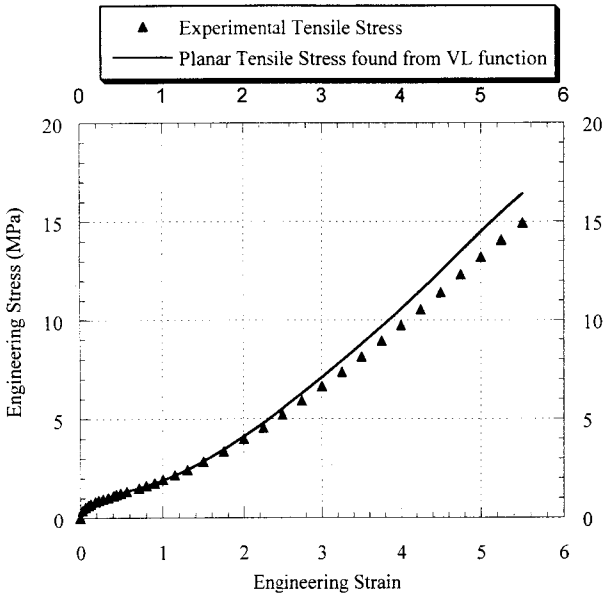

Figure 4 Comparison of the planar tensile stress–strain response calculated from the VL function for the rubber with the measured uniaxial tensile stress–strain response.

Figure 3 shows excellent agreement between the equibiaxial stresses calculated from eqs. (8) and (9).

In terms of the VL function, the planar stress–strain relationship can be expressed as follows:

$$\sigma_{\text{planar}} = u'(\lambda) - \frac{1}{\lambda^2}\, u'\left(\frac{1}{\lambda}\right) \tag{10}$$

Figure 4 is a comparison between the planar tensile (pure shear) stresses calculated from the VL function and the experimental uniaxial tensile stresses. Note that the planar stresses are slightly larger than are the uniaxial stresses at a given level of strain. The relative values are consistent with experimental data reported by Treloar.[18] This result is expected since the force required to deform a specimen in planar tension should be at least as large as is the force required in uniaxial tension because additional constraints are imposed on the specimen along the axis perpendicular to the direction of loading.

As noted above, the uniaxial engineering stress–strain data points were used to obtain the deviatoric constants for the rubber model. When only these experimental data points are used to find the constants in the polynomial and Ogden strain-energy density functions [see eqs. (2) and (5)], the model is referred to as experimental axial data (EAD). Additionally, a second data set was generated to determine the deviatoric constants and included the planar tension data calculated from the VL function and the uniaxial engineering stress–strain data points. We refer to this model as generated planar data (GPD). The hydrostatic portion of the polynomial and Ogden models remains the same, and the constants were found from the experimental pressure–volume data shown in Figure 2.

COMPARISON OF THE RUBBER MODELS IN ABAQUS

One way to verify if the generated planar tension data improve the computer model is to compare the finite-element results of the GPD and EAD models. This comparison was performed for four modes of deformation: uniaxial tension, uniaxial compression, equibiaxial tension, and planar tension.

First, we determine the number of terms needed to approximate the strain-energy density function. It is helpful to look at the reduced stress[19,20]:

$$t_R = \frac{t}{\left(\lambda^2 - \frac{1}{\lambda}\right)} = 2\left(\frac{\partial U}{\partial I_1} + \frac{1}{\lambda}\,\frac{\partial U}{\partial I_2}\right) \tag{11}$$

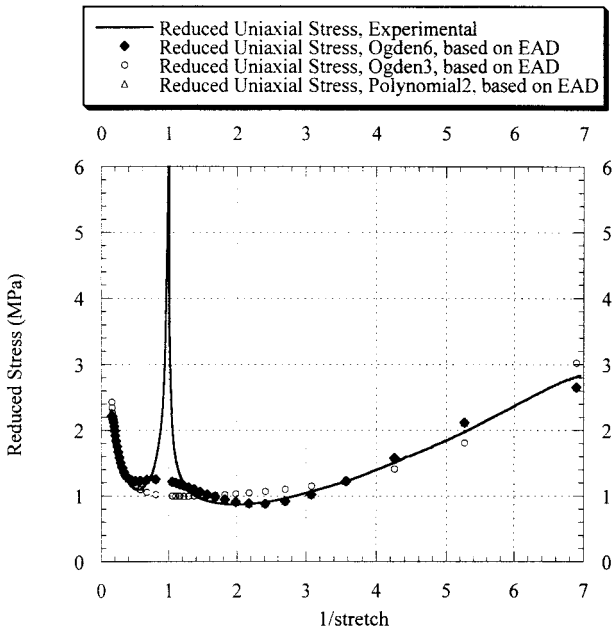

Figure 5 Comparison of the reduced stress as calculated from the different rubber models with that determined from the experimental data.

Table II Average RMS Error of Calibration Runs for Uniaxial Tension

Rubber Model		Ogden ($N = 6$)	Ogden ($N = 3$)	Polynomial ($N = 2$)
EAD	Compressible	0.0195	0.0159	0.0177
GPD	Compressible	0.0119	0.0160	0.0195

The reduced stress provides a sensitive measure of the deviations of the elastic properties from constant values.[18,20] By plotting $1/\lambda$ as the abscissa, the compression domain is the region greater than 1 and the tension domain is compressed between 0 and 1.

The polynomial strain-energy density function is shown in eq. (2). For $N = 1$, we get the Mooney–Rivlin model [see eq. (3)]. Taking the appropriate derivatives of eq. (3) and inserting them into eq. (11), the reduced stress–strain relation for uniaxial tension and compression is

$$t_R = 2C_{10} + \frac{1}{\lambda} 2C_{01} \tag{12}$$

Equation (12) shows that the Mooney–Rivlin model results in the reduced stress being linear in $1/\lambda$. Figure 5 shows the experimental uniaxial tensile and compressive data expressed as reduced stresses and plotted versus $1/\lambda$. Also shown are the results from the finite-element analysis.

For our present discussion, we look only at the experimental data. There are several points to be noted from the data. First, the behavior is unusual in two respects: At small deformations, there appears to be a large upswing in the reduced stress values as λ approaches the undeformed state. This is sometimes thought to occur because of experimental uncertainties at smaller deformations,[19] but do seem to be outside of the experimental errors here. It is possible that the result is due to the specifics of the unknown rubber compound and filler. We address this point further, subsequently. The second unusual result is the concave curvature of the behavior at high stretches and large compressions (ignoring the small-strain region). Generally, unfilled rubber does not exhibit such behavior[21] and this may be due to limited chain extensibility that is exaggerated by the presence of the reinforcing filler. The

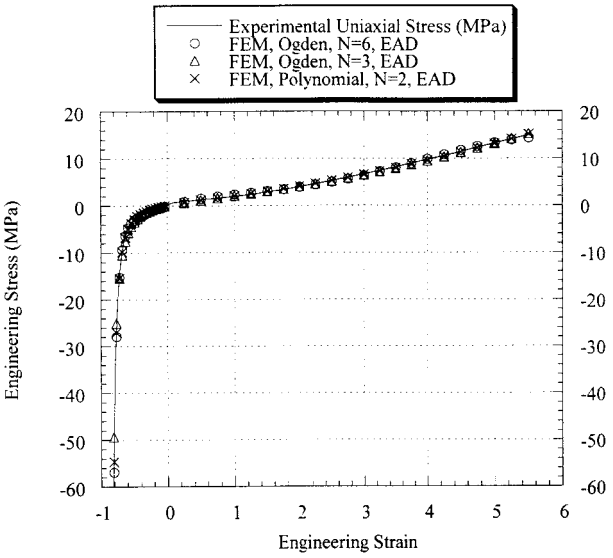

Figure 6 Comparison of the experimental uniaxial stress–strain response of the rubber with finite-element calculations for different strain-energy functions determined without using the VL function-generated data (planar tension).

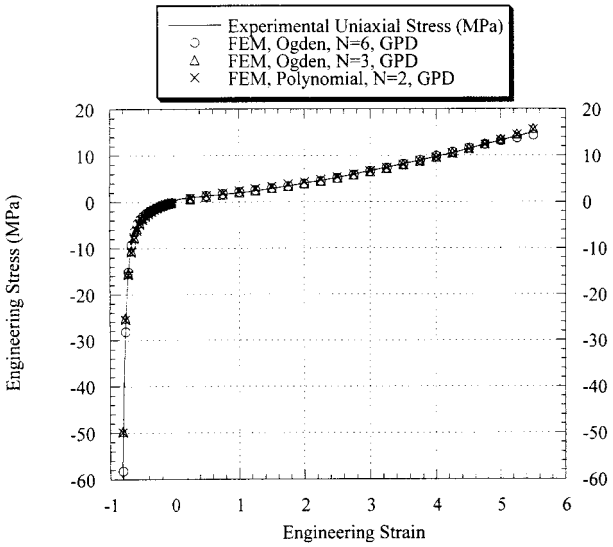

Figure 7 Comparison of the experimental uniaxial stress–strain response of the rubber with finite-element calculations for different strain-energy functions determined using the VL function-generated data (planar tension) (GPD).

Table III Average RMS Error of Calibration Runs for Uniaxial Compression

Rubber Model		Ogden ($N = 6$)	Ogden ($N = 3$)	Polynomial ($N = 2$)
EAD	Compressible	0.0280	0.0446	0.0476
GPD	Compressible	0.0305	0.0451	0.0508

origins of the behavior are beyond the scope of the current work and we do not address this point further.

The net outcome of the observations, however, is that it becomes clear that the simplest form of polynomial expression cannot describe the behavior (i.e., the Mooney–Rivlin representation). For this reason, we chose to use $N = 2$ for the polynomial strain-energy density function. This was the highest order for this function available in the version of the finite-element code used and has seven constants C_{ij}.

For the Ogden strain-energy density function, determination of the order needed ($N = 1, \ldots, 6$) to capture the nonlinearity in the experimental data is not as easy to see because the function is written in terms of the stretches. In this case, the derivative with respect to the strain invariants is not readily evaluated. We believe that using more terms should help capture the nonlinearity in the reduced stress versus the stretch curve. We used $N = 6$, which is the largest number of terms available in the finite-element code used. We also used $N = 3$ for comparison.

To compare the finite-element results against the experimental and calculated data for the three models, we calculated the average root-mean-square (rms) error. The average rms error is calculated from the formula shown in eq. (13) and measures the relative error in stress:

$$\text{avg rms error} = \frac{1}{M}\sqrt{\sum_{i=1}^{N}\left(\frac{\sigma_{\text{exp}} - \sigma_{\text{FE}}}{\sigma_{\text{exp}}}\right)} \quad (13)$$

M is the number of points at which the stress was calculated by the finite-element analysis; σ_{FE}, the stress calculated by the finite-element analysis; and σ_{exp}, the stress obtained from the experimental data.

Table II shows the average rms error for each of the calibration runs for uniaxial tension. The performance of each model is good, with slightly better results from the model based on GPD. Figures 6 and 7 are plots of the finite-element results versus the experimental uniaxial data (tension and compression). This plot graphically depicts the closeness of the finite-element approximations to the tensile data, using both experimental data and data generated by the VL function.

Table III shows the average rms error for each of the calibration runs for uniaxial compression. Each finite-element result provides a good approximation to the experimental compression data, with EAD being slightly better. Also, note that the Ogden model with six terms ($N = 6$) results in the lowest average rms error for each rubber model. In Figures 6 and 7, the compression data corresponds to strains less than zero.

Table IV shows the average rms error for each of the calibration runs for equibiaxial tension, and Figures 8 and 9 show plots of each run. The comparisons are between the data generated by the VL function and the ABAQUS results using the two rubber models. The results for each rubber model are comparable, but the experimental rubber model EAD does a slightly better job than does GPD when using the Ogden, $N = 6$, and the polynomial, $N = 2$, strain-energy density functions, with the Ogden, $N = 6$, strain-energy density function providing the best fit to the equibiaxial data generated by the VL function. It is important to note that rubber models EAD and GPD do not include the equibiaxial data set, yet the finite-element models closely approximate the equibiaxial deformation mode.

Table IV Average RMS Error of Calibration Runs for Equibiaxial Tension

Rubber Model		Ogden ($N = 6$)	Ogden ($N = 3$)	Polynomial ($N = 2$)
EAD	Compressible	0.0117	0.0271	0.0226
GPD	Compressible	0.0135	0.0273	0.0389

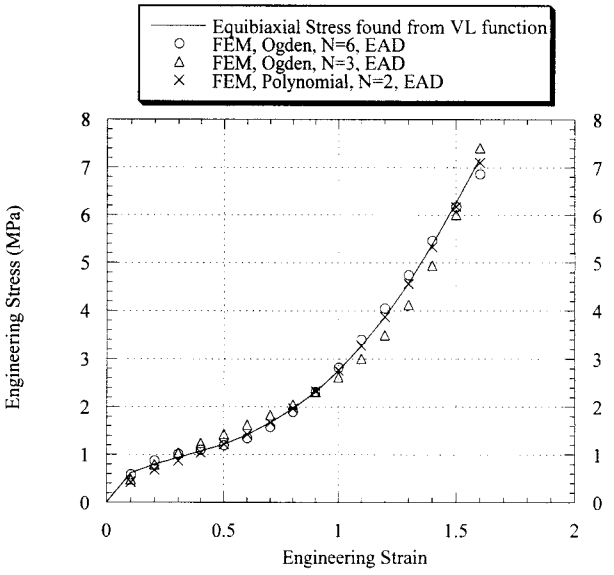

Figure 8 Comparison of the experimental equibiaxial stress–strain response of the rubber with finite-element calculations for different strain-energy functions determined without using the VL function-generated data (planar tension).

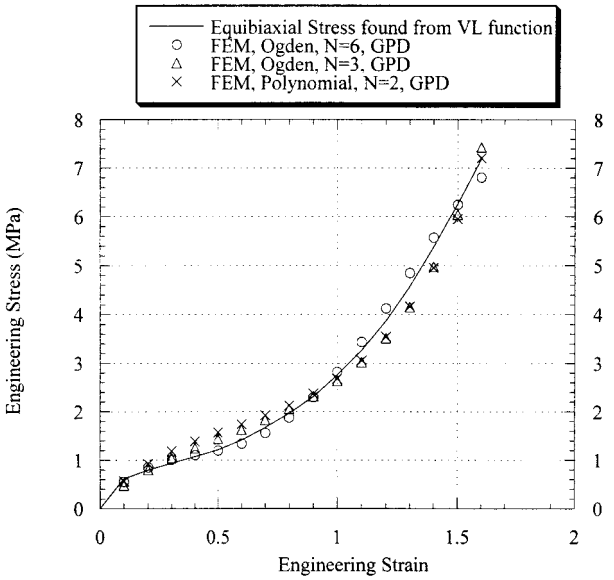

Figure 9 Comparison of the experimental equibiaxial stress–strain response of the rubber with finite-element calculations for different strain-energy functions determined using the VL function-generated data (planar tension).

Table V shows the average rms error for each of the calibration runs for planar tension, and Figures 10 and 11 show plots of each run. An important observation is that the Ogden strain-energy function, using the rubber model EAD (which does not include the planar data), does a much better job of fitting the planar data than does the polynomial strain-energy function. This is probably because the Ogden model is a special form of the VL function. A second observation is that when these calculated data are included in the data set used to determine the strain-energy density function (GPD) the polynomial strain-energy density function performs nearly as well as does the Ogden function.

As mentioned previously, the volumetric test runs were only performed using the compressibility data for rubber models EAD and GPD. Using an incompressible model would result in no deformation, since the rubber is perfectly confined. Figure 2 presents the finite-element results compared to the experimental data. The finite-element program accurately reproduces the experimental data.

Returning now to Figure 5 and the plot of the reduced stress versus for the EAD rubber model, the experimental data exhibit a rapid increase in the modulus as the unstrained state is approached. The results using the GPD data are identical. This was observed by McKenna and Zapas[19,22] and other authors. The finite-element results using the polynomial or Ogden forms of the strain-energy function do not capture this change in reduced stress. McKenna and Zapas[22] also noted that the VL function did not capture this behavior at small strains. McKenna and Zapas[19] reported that the compression modulus is greater than is the tension modulus near the undeformed state. This observation agrees with our experimental data. The reasons for this phenomenon are not clear. It is interesting to note that McKenna and Zapas[19,22] used bonded cylinders.

Table V Average RMS Error of Calibration Runs for Planar Tension

Rubber Model		Ogden ($N = 6$)	Ogden ($N = 3$)	Polynomial ($N = 2$)
EAD	Compressible	0.0182	0.0147	0.0954
GPD	Compressible	0.0100	0.0123	0.0243

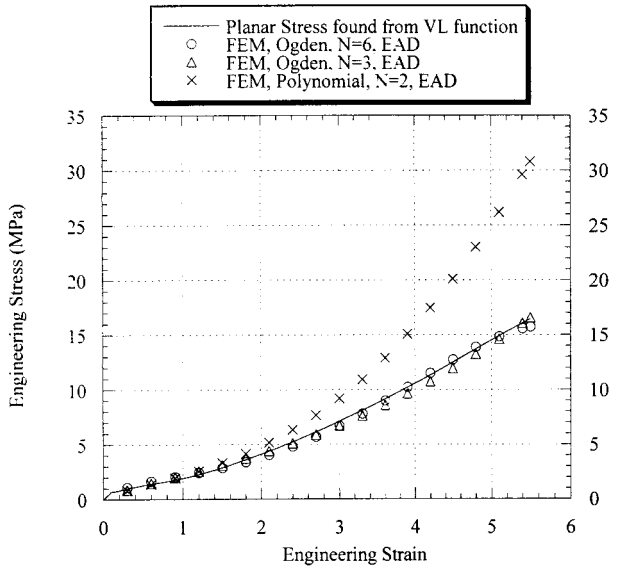

Figure 10 Comparison of the VL-calculated planar stress–strain response of the rubber with finite-element calculations for different strain-energy functions determined without using the VL function-generated data (planar tension). Note that the polynomial expansion provides a poor fit to this case.

They corrected the results to homogeneous compression using factors determined in a finite-difference analysis and conjectured that this phenomenon might be due to their experimental approach. However, in the current experiments, the tests were carried out on unbonded cylinders that had been lubricated to reduce friction along the loaded surfaces.

CONCLUSIONS

The strain-energy density function for an elastomeric material that is used in rubber bearings for earthquake isolation of buildings was determined in order that the load-deformation response of the bearing could be calculated from the hyperelastic models in the ABAQUS[1] finite-element program. Because only uniaxial testing could be performed, we used the VL function to extend the experimental rubber stress–strain data into the planar tensile (pure shear) mode. The polynomial and Ogden forms of the strain-energy function that were available in ABAQUS were then fitted to the tension and compression data and the VL expanded data set that includes planar tension. Using only uniaxial data to determine the elastic constants, the Ogden strain-energy density function, which is a special case of the VL function, was able to predict the full and expanded data set. The polynomial strain-energy density function with second-order terms ($N = 2$, corresponding to seven terms) significantly overestimates the planar tensile stresses calculated from the VL or Ogden functions. This suggests that the polynomial strain-energy density function has a different sensitivity to the test geometries used for the data input than does the VL function (or the Ogden function).

It should be noted that most work in rubber using the VL function and Mooney–Rivlin plots was done with unfilled rubber. However, the rubber used in this testing program is filled with carbon black, typical of most structural uses of rubber (tires, elastomeric bearings, etc.). The Mooney–Rivlin plots of unfilled rubbers exhibit different behavior from that observed here.[21] With unfilled rubbers, the response starts at a low value, goes toward a maximum in the vicinity of $1/\lambda = 1$, and then decreases mildly before, possibly, increasing again. Here, the response at values of $1/\lambda$ increases at a rapid rate.

The authors gratefully acknowledge partial support of this work by the Building and Fire Research Labora-

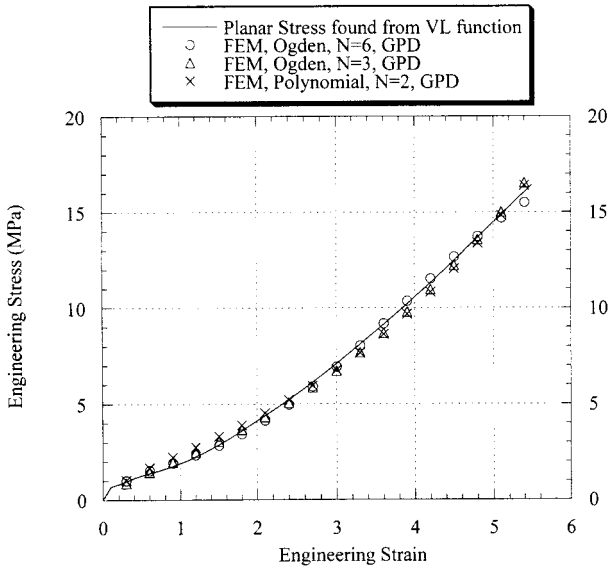

Figure 11 Comparison of the VL-calculated stress–strain response of the rubber with finite-element calculations for different strain-energy functions determined using the VL function-generated data (planar tension). Note: Compare the improvement of the polynomial expansion fit to the data.

tory and the Materials Science and Engineering Laboratory of the National Institute of Standards and Technology in Gaithersburg, Maryland.

REFERENCES

1. ABAQUS/Standard Users Manual, Version 5.5; HKS, Inc., 1995.
2. Bradley, G. L. Master's Thesis, University of Maryland, 1997.
3. Valanis, K. C.; Landel, R. F. J Appl Phys 1967, 38, 2997–3001.
4. Walter, J. D. Rubb Chem Technol 1978, 51, 524–576.
5. Peng, S. H.; Chang, W. V. Comput Struct 1997, 62, 573–593.
6. Chen, J. S.; Pan, C. J Appl Mech 1996, 63, 862–868.
7. Penn, R. W. Trans Soc Rheol 1970, 14, 509–517.
8. Fong, J. T.; Penn, R. W. Trans Soc Rheol 1975, 19, 99–113.
9. Sussman, T. S.; Bathe, K .J. Comput Struct 1987, 26, 357–409.
10. Vangerko, H.; Treloar, L. R. G. J Phys D Appl Phys 1978, 11, 1969–1978.
11. Glucklich, J.; Landel, R. F. J Polym Sci 1978, 15, 2185–2199.
12. McKenna, G. B.; Flynn, K. M.; Chen, Y.-H. Macromolecules 1989, 22, 4507–4512.
13. Kearsley, E. A.; Zapas, L. J. J Rheol 1980, 24, 483–500.
14. ASTM D 3182-89 (Reapproved 1994), Standard Practice for Rubber—Materials, Equipment, and Procedures for Mixing Standard Compounds and Preparing Standard Vulcanized Sheets.
15. ASTM D 395-89 (Reapproved 1994), Standard Test Methods for Rubber Property—Compression-Set.
16. Gent, A. N.; Lindley, P. B. In Proceedings of the Institution of Mechanical Engineers, 1959; Vol. 173, pp 111–117.
17. Ketcham, S. A.; Niemiec, J. M.; McKenna, G. B. Eng Mech 1996, 122, 669–677.
18. Treloar, L. R. G. Trans Faraday Soc 1943, 40, 59–70.
19. McKenna, G. B.; Zapas, L. J. Polymer 1983, 24, 1502–1506.
20. Yeoh, O. H. Rubb Chem Technol 1993, 66, 754–771.
21. Han, W. H.; Horkay, F.; McKenna, G. B. J Math Mech Mater 1999, 4, 139–167.
22. McKenna, G. B.; Zapas, L. J. Rubb Chem Technol 1986, 59, 130–137.